
PJB
MAITENANCE REPAIR OVERHAUL SOLUTION :
Steam Turbine Rotor Disc Failure & Repair
Prepared by :
DR. Ir. Triwibowo MSC
PT INDOCOR REKAYASA TEKNOLOGI &
B2TKS BPPT
JAKARTA / SERPONG : 3 – Desember 2020
AVAILABILITY 90+
PROPER EMAS 2017 2018 2019
MALCOLM BALDRIGE INDUSTRY LEADER

KATA PENGANTAR

- Maintenance Repair Overhaul Solution menjadi kunci penting untuk pengoperasian Pembangkit Energi Listrik yang Reliable, Safe, Optimum, Efficient dan Economical in Nature.
- Umur Plant telah banyak yang melewati 15 tahun, secara alamiah terjadi aging pada material komponen2 stationary maupun rotary.

- Peran MRO jelas menjadi sangat penting bahkan vital untuk mendapatkan kondisi operasi yang reliable, safe, effisient optimum namun tetap ekonomis. Sementara itu ketersediaan dana untuk spare parts replacement sangat dibatasi
- Dalam kondisi Pandemi Covid-19, jelas sekali pasokan listrik tidak boleh terganggu untuk menjaga semua kegiatan

Masyarakat Umum dan Pemerintah agar tetap berjalan normal dan lancar.

- Sebagai contoh kasus adalah bila terjadi kerusakan fatal pada disc dari steam turbine rotor, maka opsi rotor turbine repair harus dipertimbangkan mengingat dana untuk pembelian rotor baru belum tentu tersedia.
- Pembahasan MRO untuk steam turbine rotor disc ini sengaja diberikan dalam Bahasa Inggris untuk latihan diskusi dalam atmosphere international.

I. INTRODUCTION.

- Rotor steam turbine was purchased in 2005, then it was carefully stocked until November 2017.

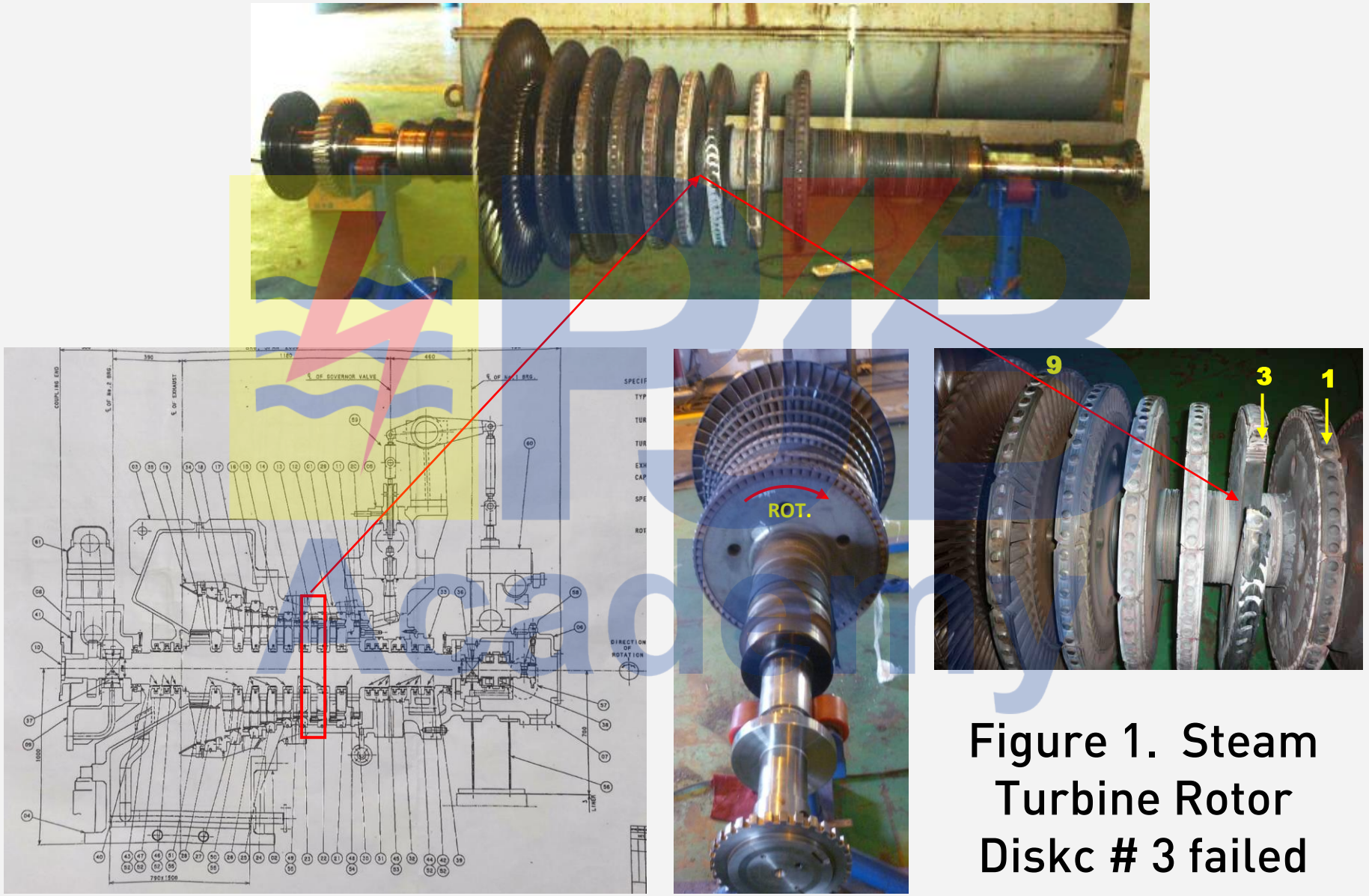

Figure 1. Steam Turbine Rotor Diskc # 3 failed

- In November 2017 the steam turbine rotor was installed and operated.
- Alarm sounded on 23th- Agustus 2020 at 05:20:41 a.m. (see recorded data). Steam turbie trip took place at 05:33:17.
- Steam turbine rotor disc no. 3 was damaged / broken.
- It is required to find out the root cause of the rotor disk failure, so that appropriate measures can be taken

II. TECHNICAL DATA

Item	:	Steam turbine
Disc Turbine Material	:	AISI 4130
Dimension	:	See technical drawing
Service	:	Steam
Steam Temp.	:	390-400 °C
Capacity	:	- Rated 7020 KW
		- Normal 6030 KW
Steam Pressure Inlet	:	Normal 92.5mmHg A
Design	:	Mitsubishi Heavy Industries Ltd.

III. TESTING

- VISUAL
- MACROFRACTOGRAPHY
- METALOGRAPHY
- HARDNESS TEST
- STEAM TURBINE DISC CHEMICAL COMOSITION TEST
- SEM/EDS

IV. RESULTS AND DISCUSSION

FACTS :

- High cycle fatigue with low nominal tensile stresses
- No surface damages due to corrosion nor mechanical impacts
- Initial defects

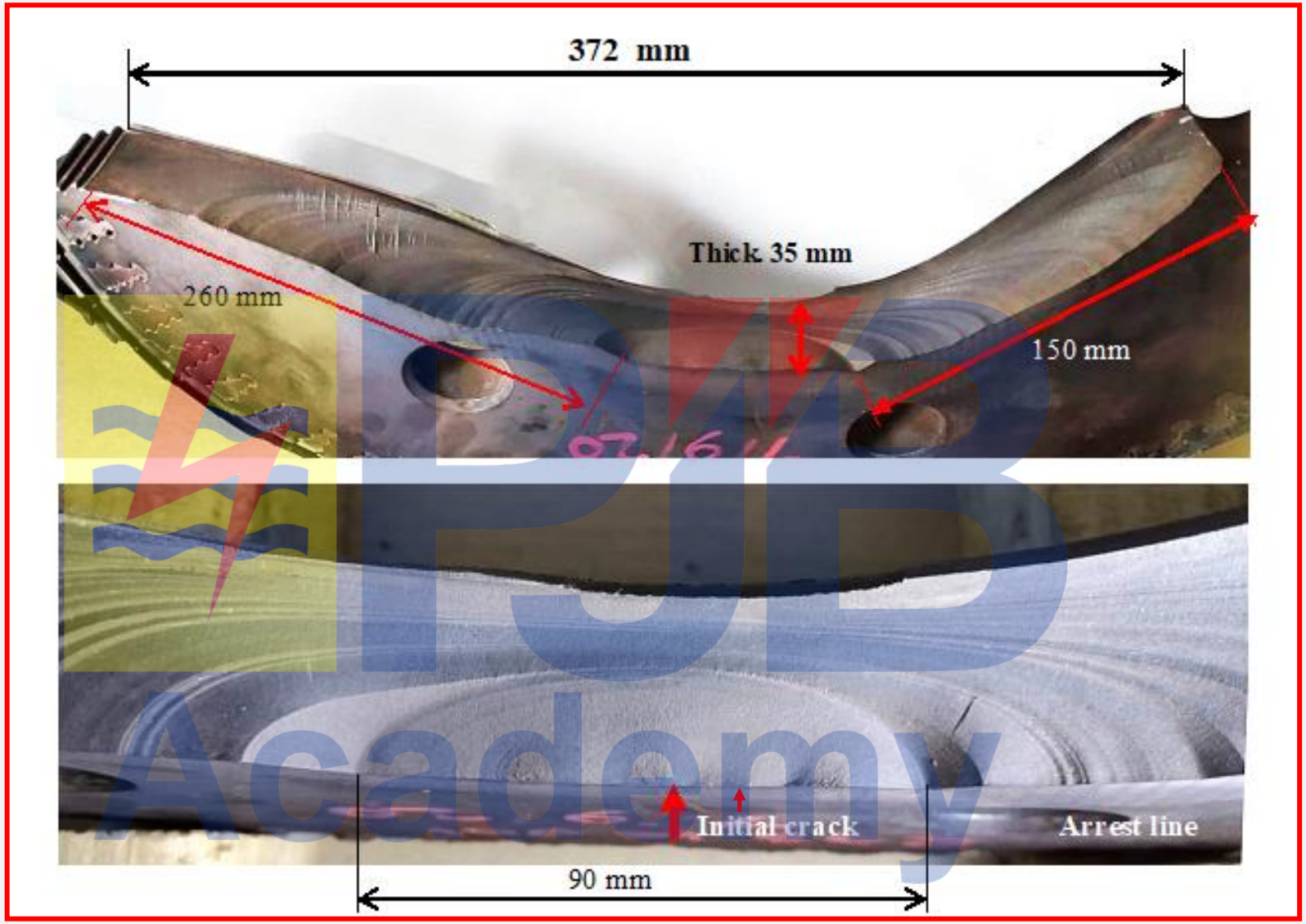

- Fatique fracture characterized by beach marks.
- 98 % fatigue area and around 2 % static overload failure / final fracture.
- Multiple fatigue initiation.

- Critical areas of the rotor are on the fillet and bore position
- Fatigue took place on rotor disc #3

HYPOTHESES :

- Clearly, there must be stress raisers exist on the rotor disc # 3.
- The suspected stress raisers are very likely material defect


11/23/2020
1:28:36 PM
det
ETD
pressure
2.09e-3 Pa
HV
10.00 kV
mag
150 x
WD
10.5 mm
spot
3.5
HFW
847 µm
200 µm
Cipta Mikro Material

- Initial Defects in 3-dimension is likely big enough that stress intensity factor (ΔK_I) exceeds the threshold value (ΔKth).
- Consequently, fatigue crack propagation taking place during around 3 years steam turbine operation until rotor disc #3 failure.
- If no initial defects exist, then the rotor disc will not develop fatigue crack propagation within 3 (three) years only during steam turbine operation.
- Rotor manufacturer guests SCC is the root cause of the rotor disc failure.

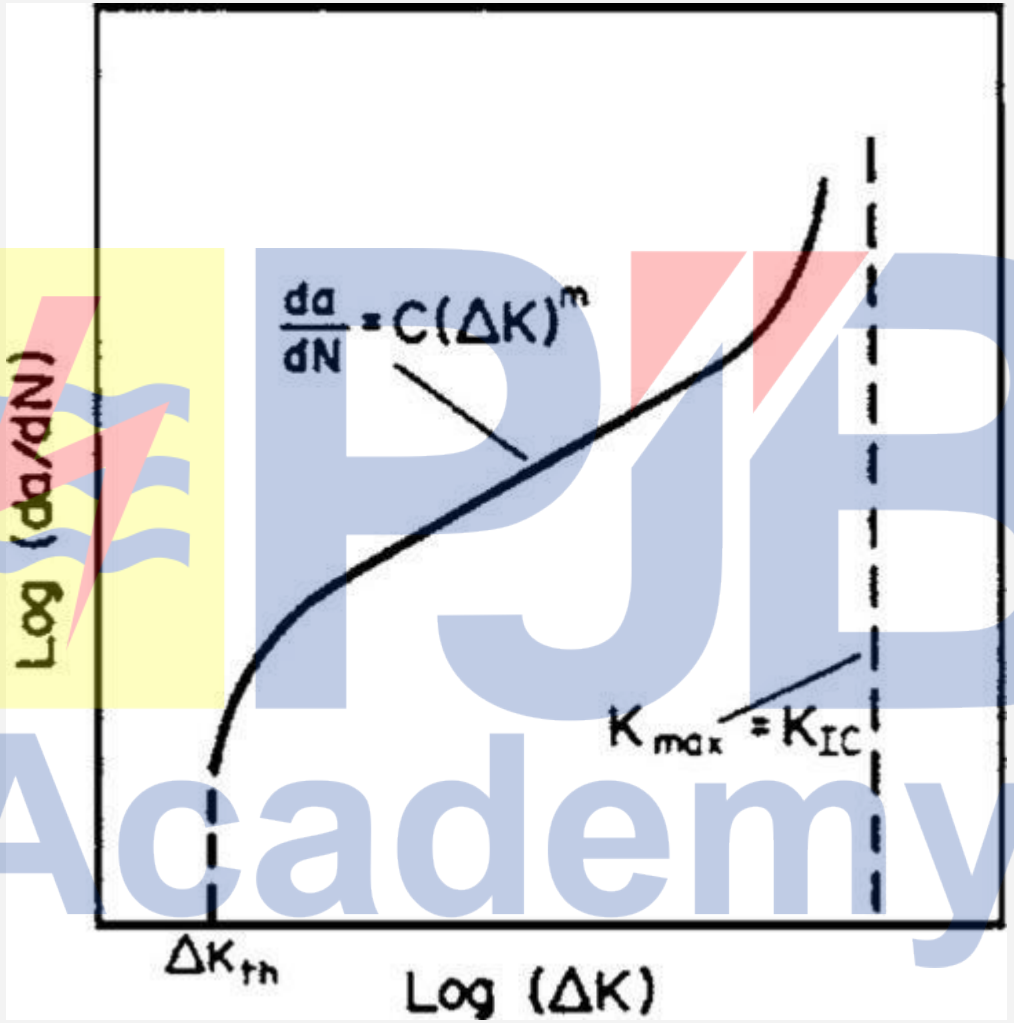

Idealised crack growth rate plot for a constant load amplitude.

Typical SCC attack, but NO evidences are found on the broken rotor disc #3

CONCLUSION & SUGESTIONS

- Root cause of rotor disc #3 failure is high cycle fatigue with low nominal load.
- Initial defects which developed into fatigue crack propagation is most likely due to material defects, because no evidences of any corrosion attack (including SCC) nor mechanical impact.
- Non Destructive Inspection before rotor installation.
- Review QA/QC new rotor production

- Install brand new rotor or :
- Repair of the broken rotor disc can be considered.

- Sensor proximity addition between blade tips and casing can detect early such a fatigue crack propagation.
- Non Destructive Inspections (NDI) by means of Penetrant Test (PT) and Magnetic Particle Test (MT) can be used as selection tool. Meanwhile, angled ultrasonics probe (PAUT type) can be chosen for defect confirmation as well as defect size measurement whenever such an indication is found.

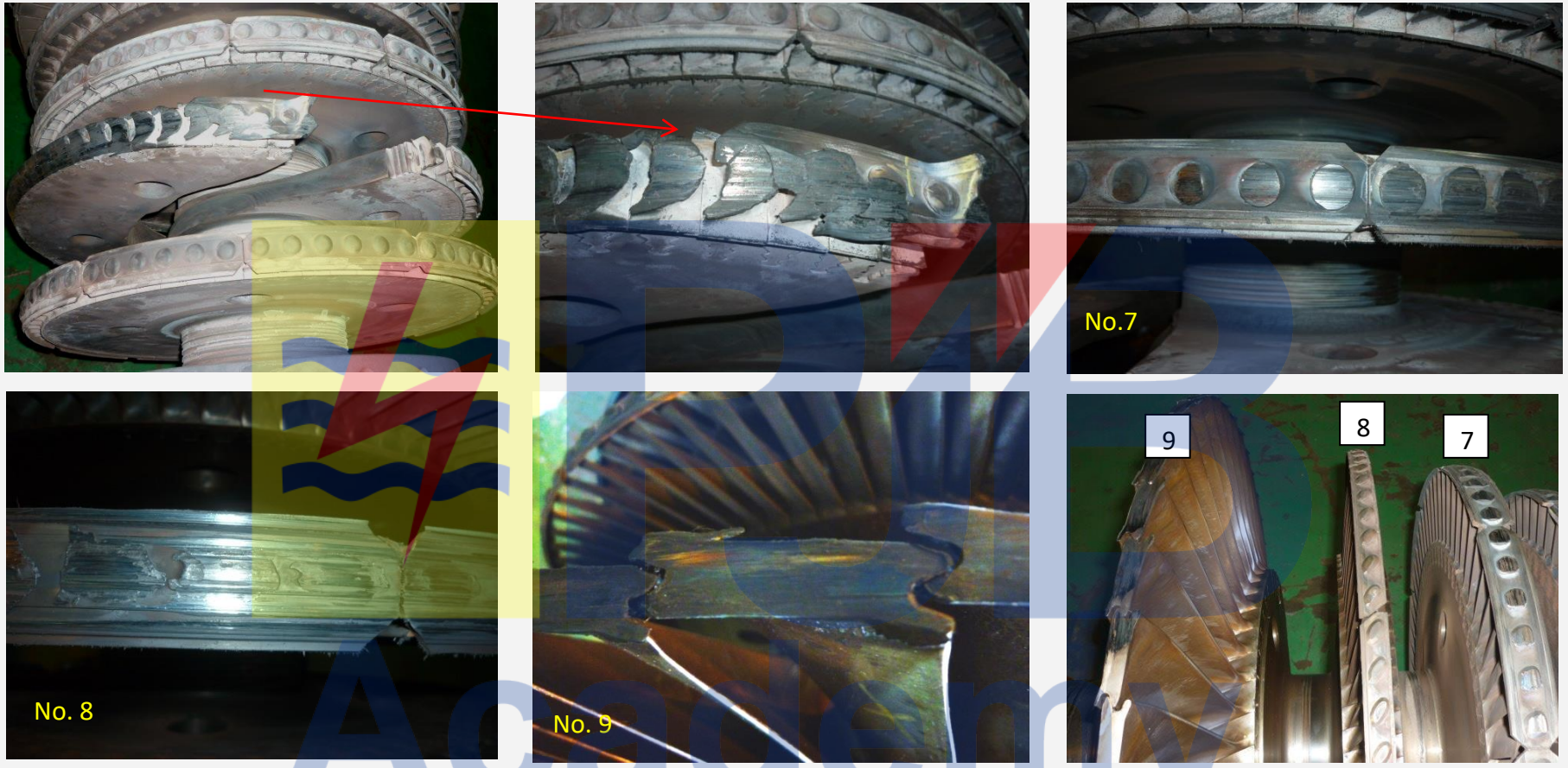

Gambar 2. Kerusakan yang ditimbulkan saat terjadinya patah pada disc No. 3 dampaknya mengakibatkan kerusakan pada rotor No. 4 sampai dengan rotor No. 9 dan pada komponen lainnya.

Gambar 3. Dilakukan pemotongan dengan las *acytilen* pada bagian rotor disc no.3. Terlihat permukaan patahan berupa patah lelah *(Fatique fracture)* yang sangat halus dan luas, hal ini dapat dilihat dengan adanya alur garis pantai ***(Beach mark)*** di seluruh permukaan patahan. Bentuk permukaan patah lelah yang sangat luas dapat digolongkan tipe low nominal stress dan tension-compression.

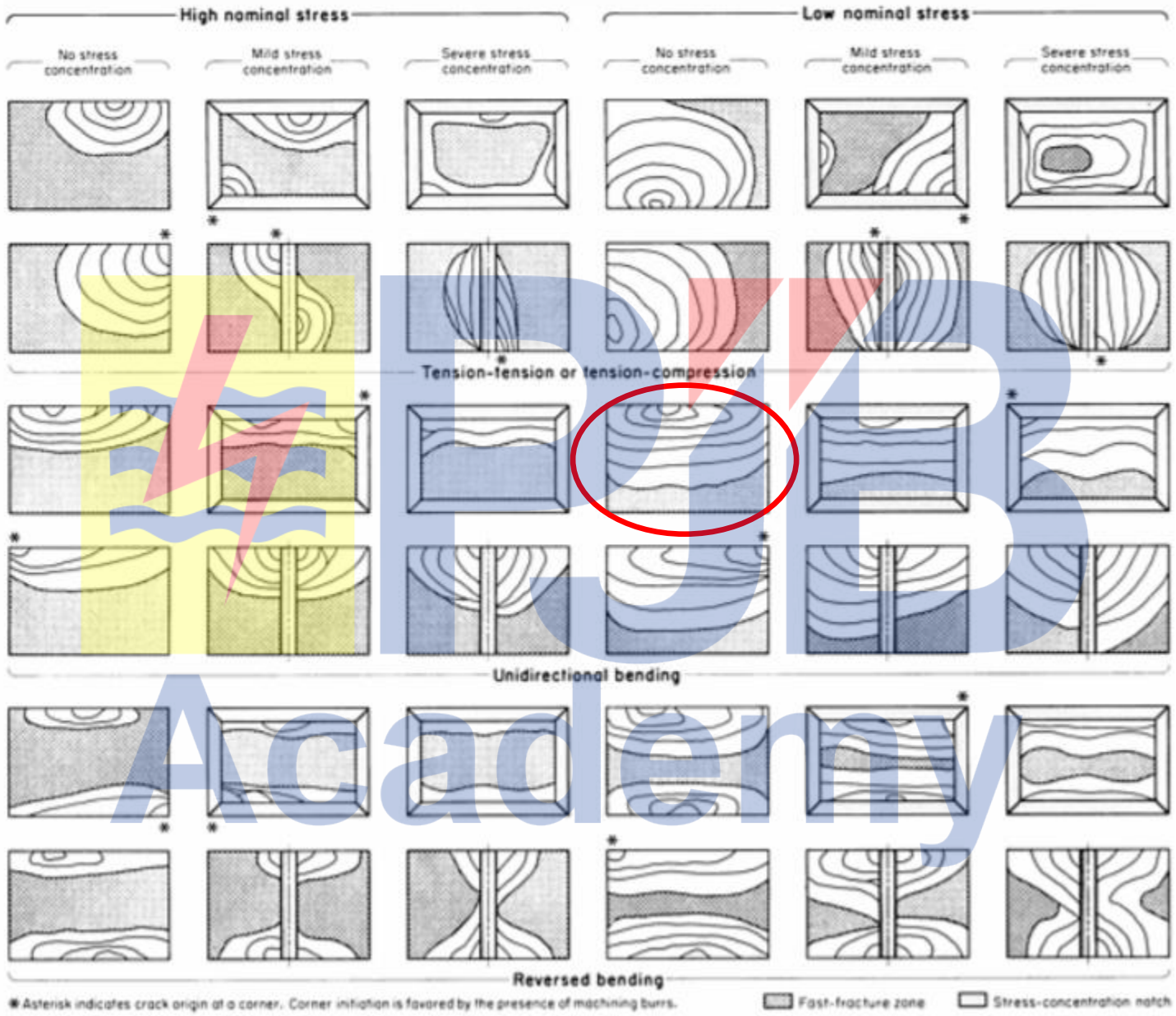

Fig. 49 Schematic representation of fatigue fracture surface marks produced in square and rectangular components and in thick plates under various loading conditions

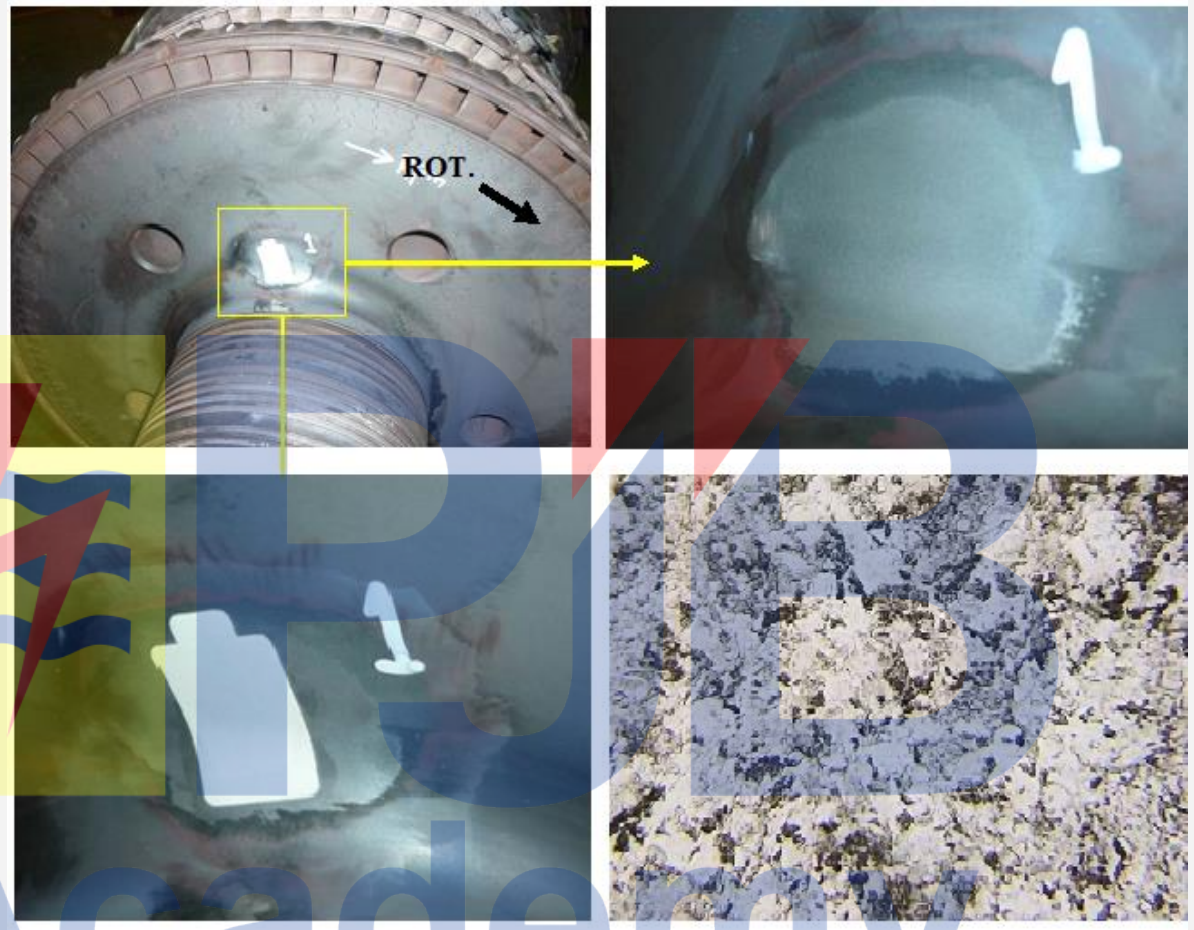

- Pemeriksaan visual dilakukan pada daerah radius disemua rotor disc tidak ditemukan adanya cacat atau retak.
- Didaerah radius dilakukan pemeriksaan metalografi, guna mengetahui adanya sambungan las fabrikasi (rotor disc no.1 yg sejajar dg rotor disc yg patah.).
- Pemeriksaan visual pada makro etsa tidak ditemukan adanya cacat atau sambungan las. Strukturmikro ferrite (putih)-pearlite.

4.4. Chemical composition test result

The following table shows the result :

	C	Si	Mn	P	S	Cr	Mo	Ni
1	0.266	0.292	0.426	0.0094	0.0061	0.436	0.556	2.79
2	0.280	0.317	0.453	0.0098	0.0062	0.445	0.656	2.78
3	0.289	0.308	0.413	0.0089	0.0073	0.438	0.576	2.79
Rata Rata	0.279	0.306	0.431	0.0094	0.0065	0.440	0.596	2.79
10325 GP	0.35 Max	0.15 Min	0.45 Min	0.015 Max	0.015 Max	0.20	0.45	2.5
4130	0.28-0.33	0.15-0.35	0.4-0.6	0.035 Max	0.04 Max	0.80-1.10	0.15-0.25	

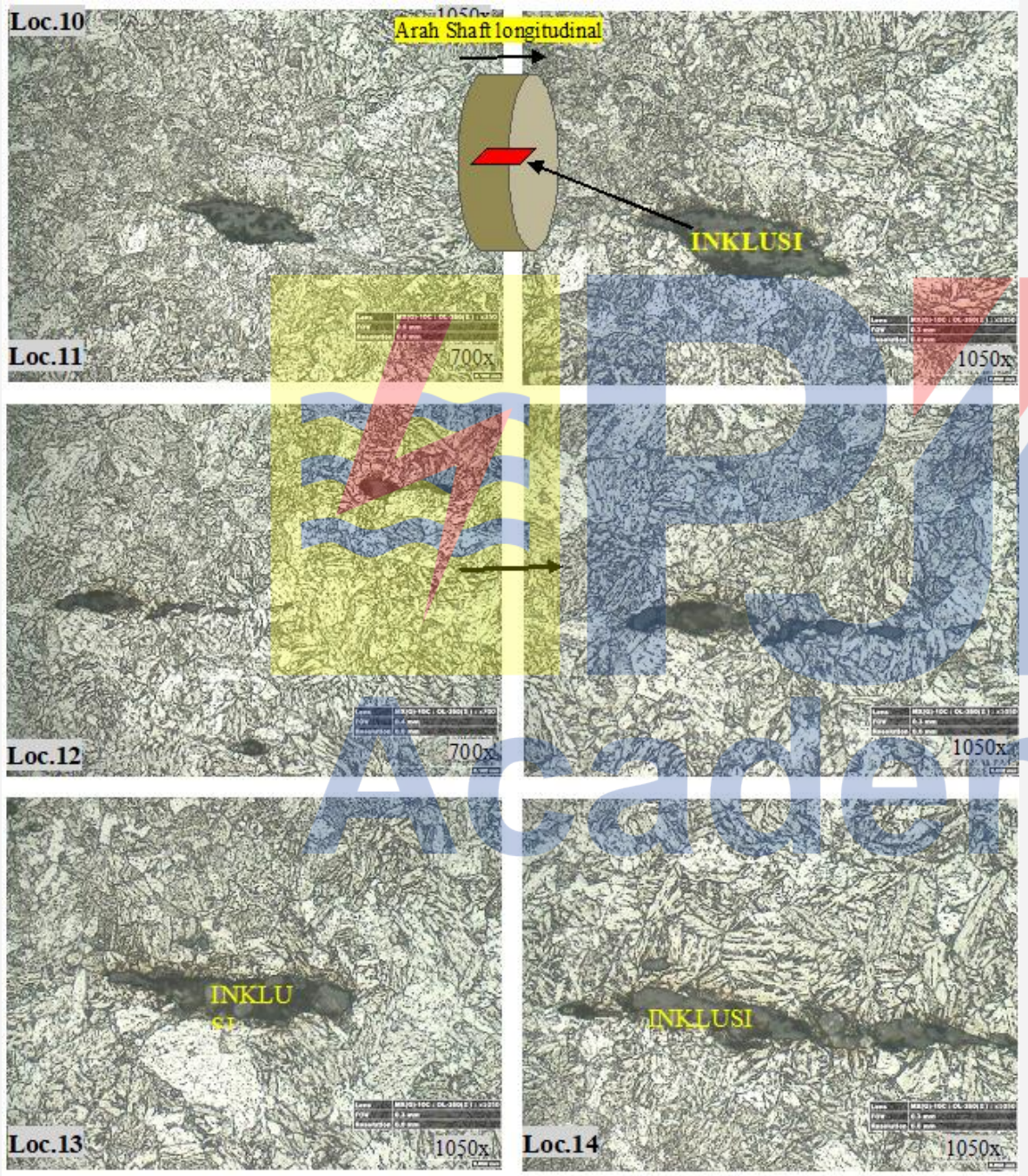

lokasi. 11, 12, 13, 14 dan 15

Hasil pemeriksaan metalografi struktur mikro berupa bainite. Selain itu ditemukan adanya INKLUSI (unsur pengotor) umumnya Mangan Sulfida dengan posisi sejajar arah shaft. Inklusi terlihat sangat panjang.

HARDNESS TEST RERESULT OF ROTOR DISC

- Machine : Frank Finotest
- Test Metode : Hardness Vickers (HV)
- Force (F) : 5 Kgf
- Identor : 136°
- Time : 15 detik
- Test Standar : SNI 19-0407-1989

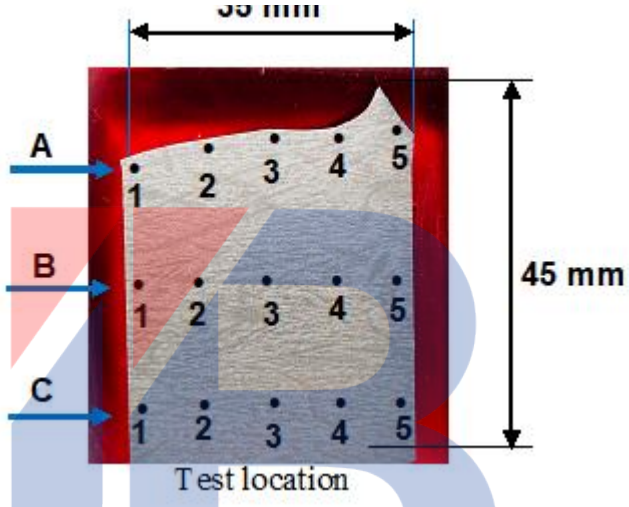

Test location

NOMOR	HARDNESS VALUE, HV			AISI 4130
	A	B	C	
1	280	282	286	207 HV
2	271	275	265	
3	265	268	274	
4	265	277	277	
5	285	282	280	
Average	273	277	276	

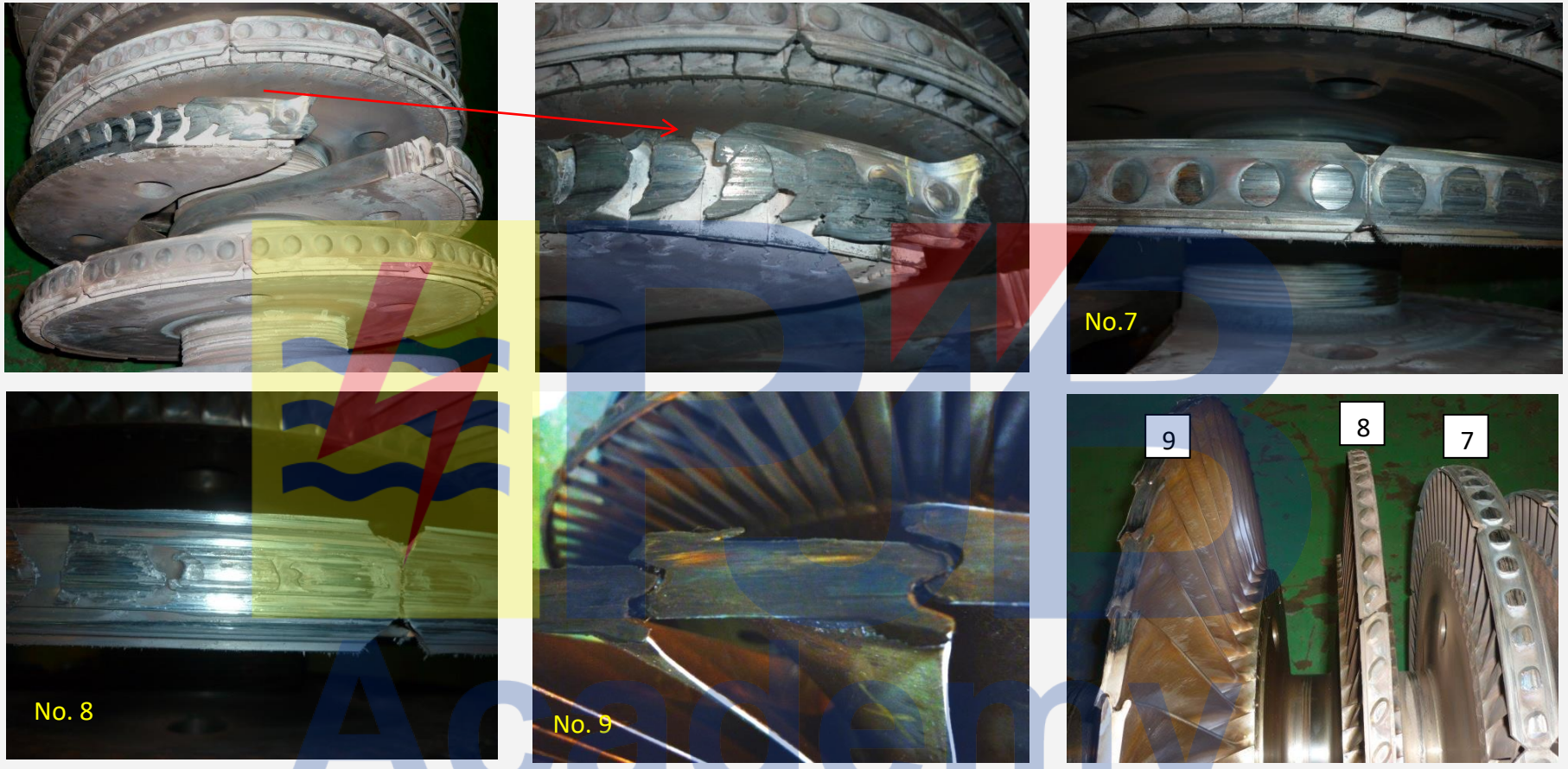

Gambar 2. Kerusakan yang ditimbulkan saat terjadinya patah pada disc No. 3 dampaknya mengakibatkan kerusakan pada rotor No. 4 sampai dengan rotor No. 9 dan pada komponen lainnya.

SEM-EDS Result (AA-169-003)

- No significant corrodant is found on the fracture surface.

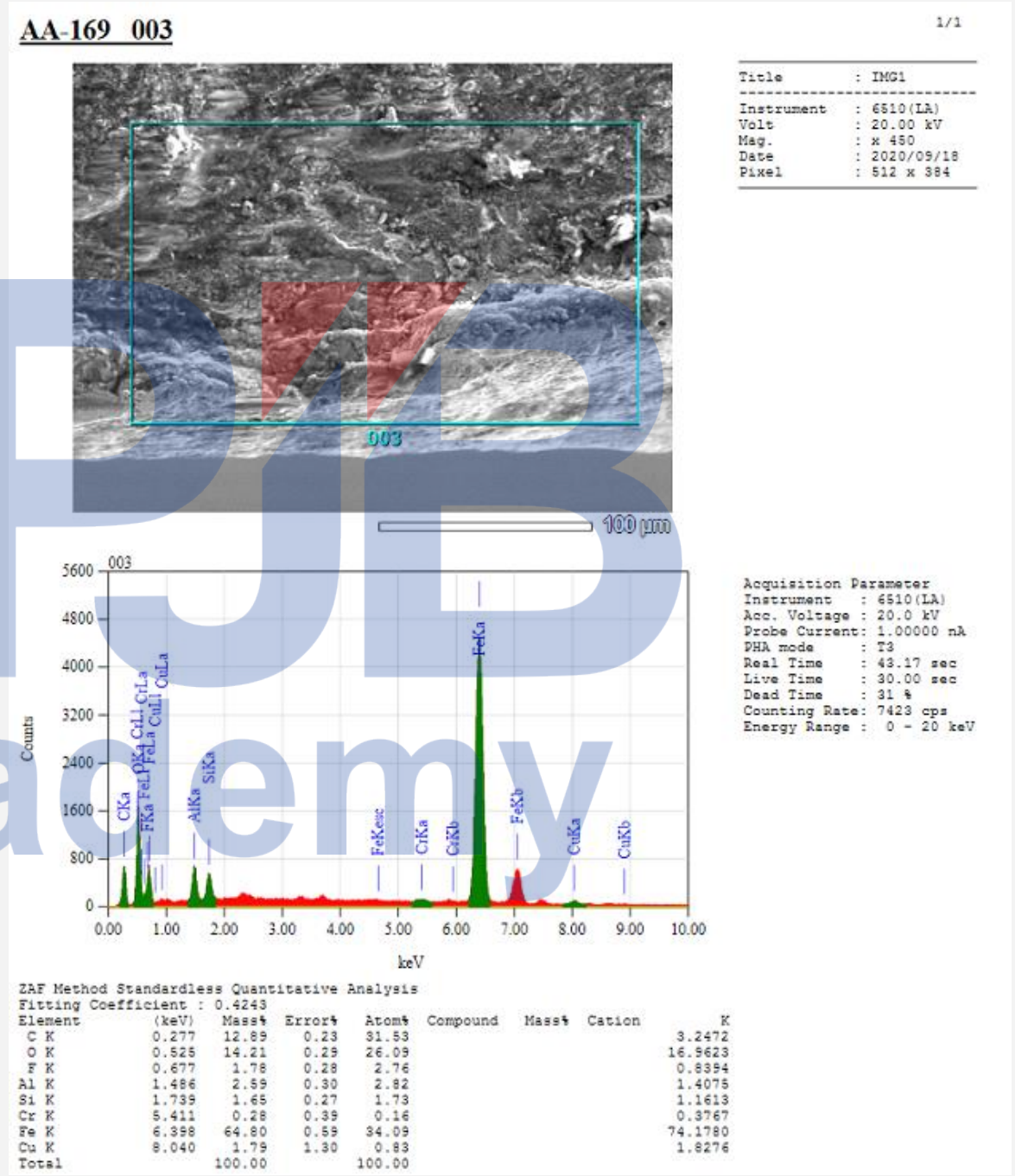

Element	(keV)	Mass%	Error%	Atom%	Compound	Mass%	Cation	K
C K	0.277	12.89	0.23	31.53				3.2472
O K	0.525	14.21	0.29	26.09				16.9623
F K	0.677	1.78	0.28	2.76				0.8394
Al K	1.486	2.59	0.30	2.82				1.4075
Si K	1.739	1.65	0.27	1.73				1.1613
Cr K	5.411	0.28	0.39	0.16				0.3767
Fe K	6.398	64.80	0.59	34.09				74.1780
Cu K	8.040	1.79	1.30	0.83				1.8276
Total		100.00		100.00				

Repair method is given in the next ppt slides :

Steam Turbine Rotor Discs Failure Evaluation and Repair Process Implementation

Source: Zdzislaw Mazur , Alejandro Hernandez-Rossette
Instituto de Investigaciones Electricas, Reforma 113, Palmira, 62490 Cuernavaca, Morelos, Mexico

Surabaya, 3 Desember 2020

Abstract

The following case of rotor disc welding repair can be used as repair reference.

Two rotor discs failed in a 84-MW unit installed in a power plant. The failure was evidenced by large circumferential fractures of blades attachments in both discs. Disc failure was evaluated by investigating rotor operation history, steady state stress analysis by finite element (FEA), disc fracture surface fractography and deposit evaluation. It was found that this disc failure was driven by stress corrosion due to significant static stresses, humid ambient operation and disc material susceptibility. To correct disc failure and restore turbine original characteristics, a disc welding repair procedure was developed. This repair process was implemented and rotor discs restored by weld deposition, post weld heat treatment and machining. As a result, the rotor was returned to service and its useful life extended.

I. Introduction

Rotor repair through welding is one of the principal means for extending rotor life. Repair processes are classified into different classes including weld build-up of gland seals and bearing journals, weld restoration of individual rotor steeples, weld build–up of rotor wheel rims, repair of circumferential cracking, replacement of rotor and welding sections in new blade ring forgings.

This paper describes a case history of the failure evaluation and repair process of stress-corrosion damaged 84-MW steam turbine rotor by means of weld built up.

II. Methodology

The rotor under evaluation corresponds to an 84-MW, 3600 rpm steam turbine. This unit has a flow high/intermediate/ low-pressure turbine composed of 13 stages of blades. This turbine had accumulated 332,000 operation hours (40 years) to failure. A turbine rotor general view is shown in Fig. 1. The failures occurred in stages L-3 and L-4 which are grouped in 6 and 5 blades, as indicated by arrows. Fig. 2 shows axial cracks in the L-3 and L-4 stage disc blade grooves, and Fig. 3 shows circumferential cracks in these same grooves. The circumferential cracks extend to approximately 350 mm in both stages.

Turbine catastrophic failure would probably occur at some future time due to blades breaking off. The rotor was made of forged low alloyed NiCrMoV steel, approximately corresponding to ASTM A-471 class 3 materials.

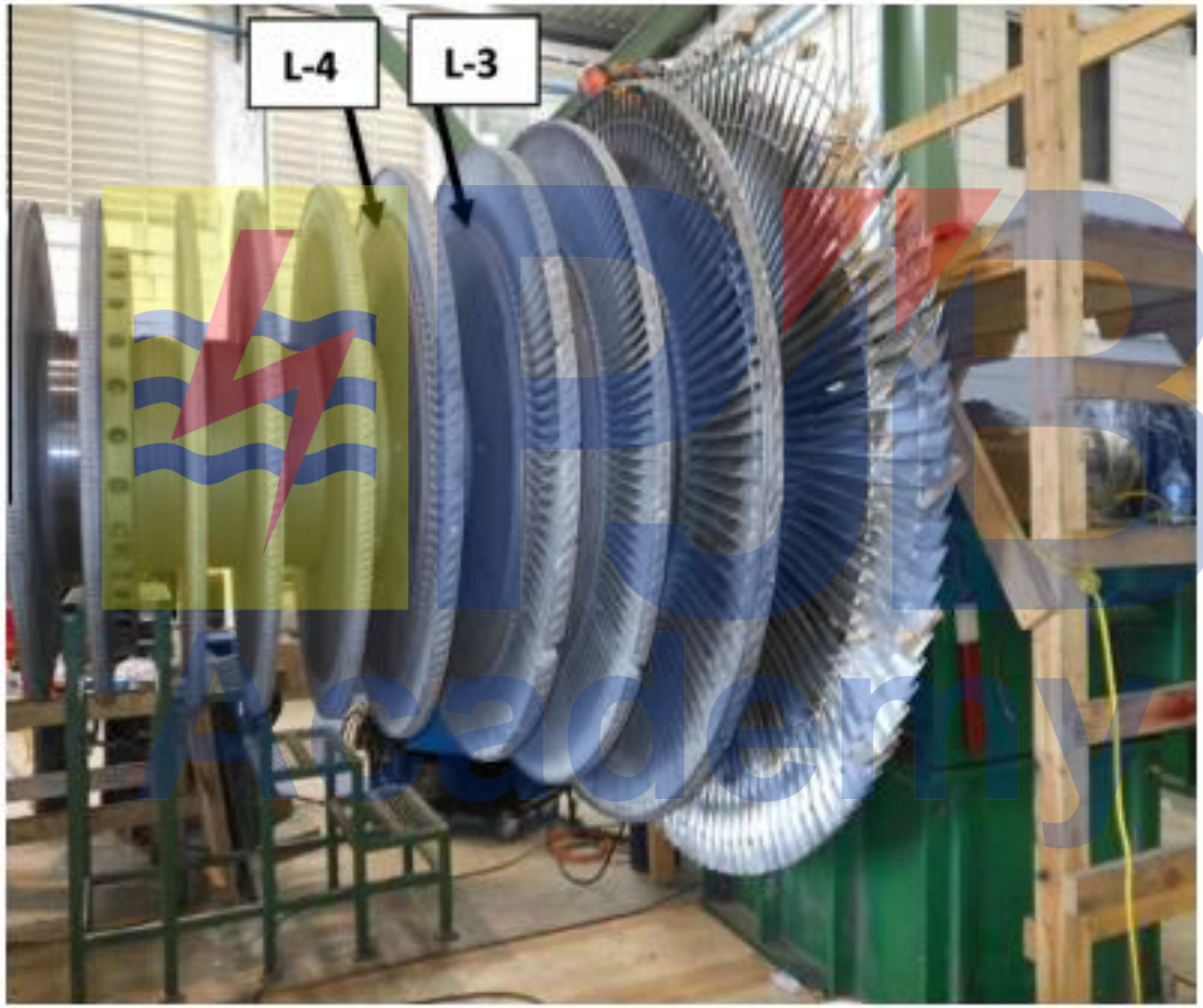

Fig. 1. General view of the rotor of the 84 MW steam turbine; the arrows indicate failed discs.

Fig. 2. Axial cracks in the blade grooves.

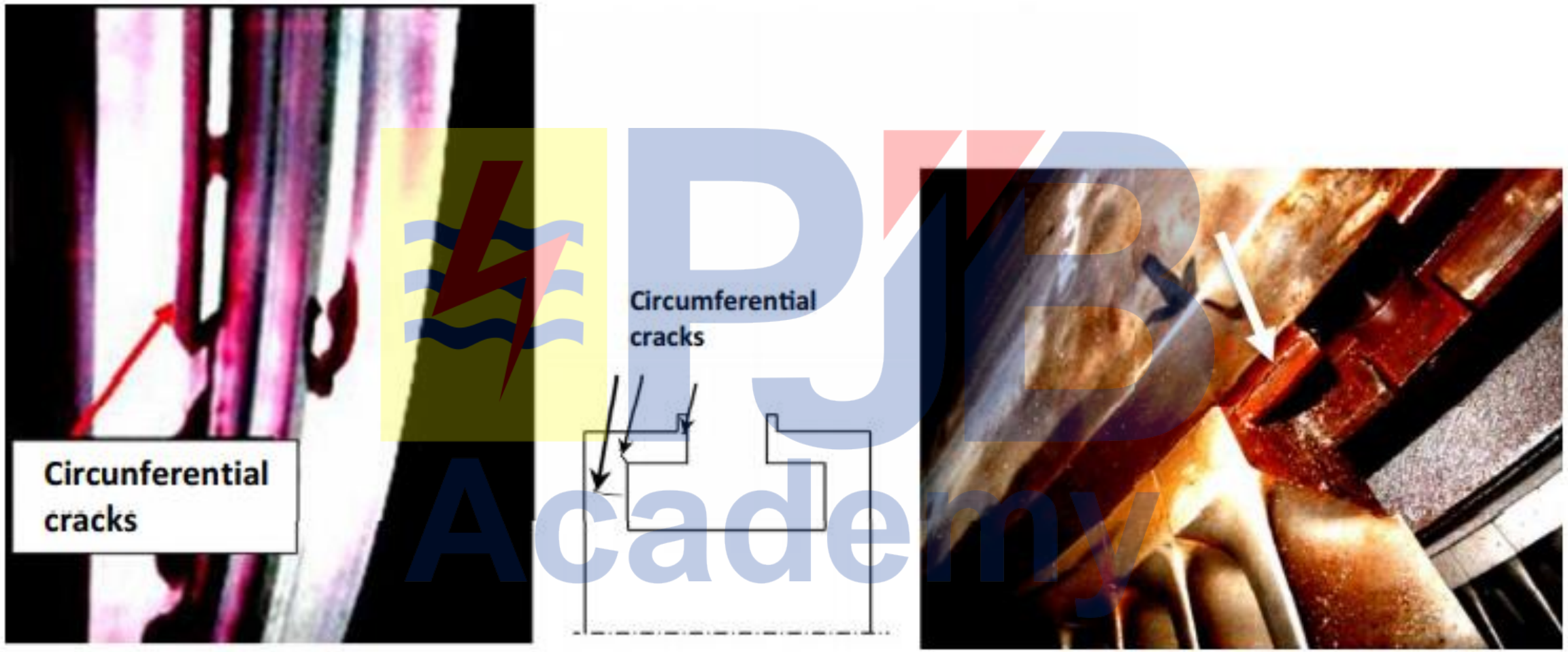

Fig. 3. Circumferential cracks in the blade grooves.

Disc Stress Analysis

III. Disc Stress Analysis

Disc static stress calculation

Disc static stress analysis included stress developed by blade centrifugal force. By applying rotor rotational velocity, centrifugal acceleration was calculated and stresses were calculated considering blade distributed mass.

Von Misses stress contours on the disc groove due to centrifugal force of the blades are shown in Fig. 5. Maximum stresses localized in the disc blade groove reached a value of Ra = 367 MPa as shown in Fig. 5. In the legend of Figs. 5 and 6 appears maximum stress of 428.6 MPa which correspond to maximum stress of L-4 stage blade which was removed from figures to see detail of disc stress distribution. The detail of maximum stress distribution on the L-4 disc is shown in Fig. 6. The rotor maximum stress is lower than the rotor material yield strength (R0.2Y.S. = 689 MPa) and the safety factor is (1.88) which is moderate.

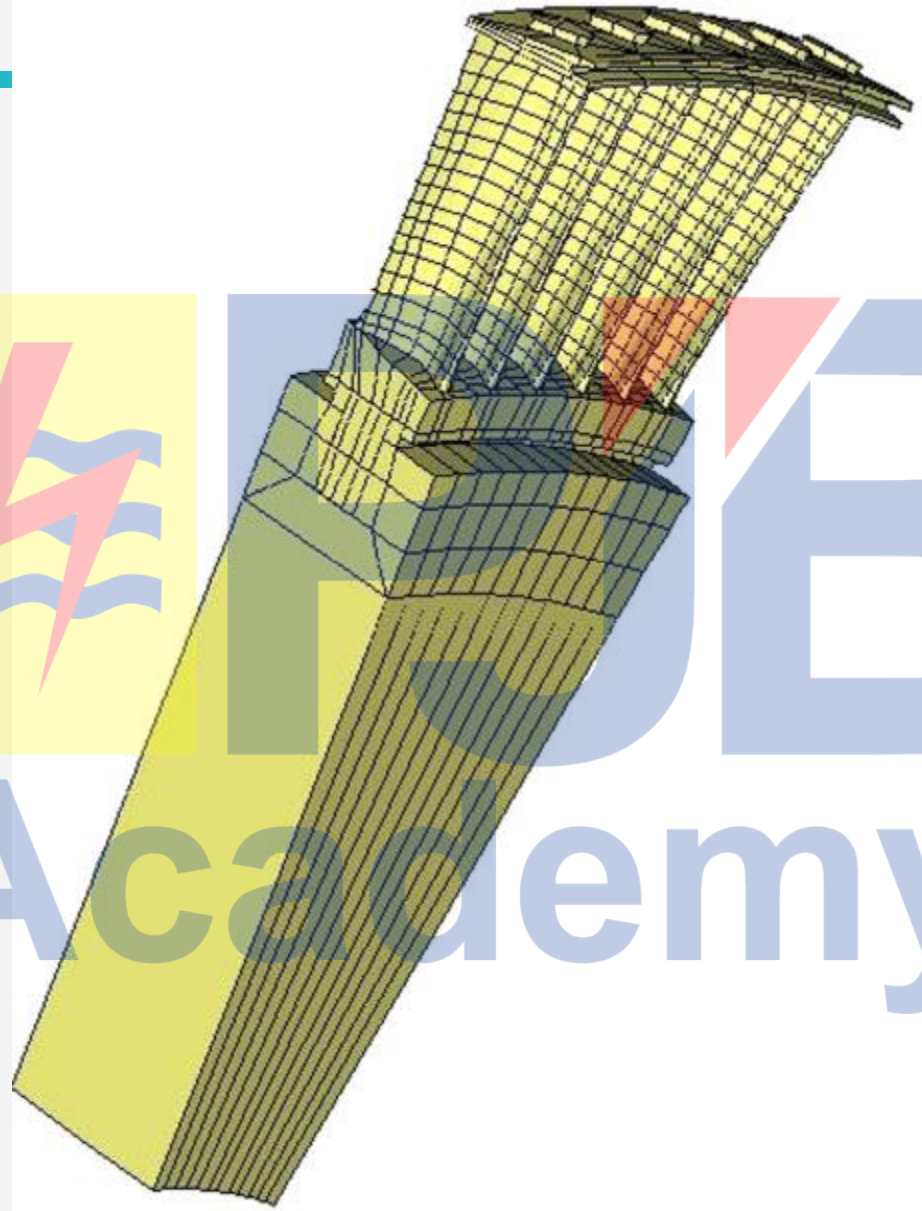

Fig. 4. Model of an L-4 stage disc segment (group of 6 blades).

IV. Rotor Disc Metallurgical Investigation

A metallurgical investigation of the failed rotor discs (L-3 and L-4) was carried out, including metallography, SEM (scanning electronic microscopy), fractography and chemical analysis. The general aspect of disc fracture surface is shown in Fig. 7. The microstructure of the rotor disc consists of fine grained bainite typical for forged low alloyed steel according to Specification ASTM A 471 cl 3. Grain sizes were ASTM 7 and 8 on average [8]. It was previous austenite grain size. Chemical composition and hardness tests were carried out on failed discs, which confirmed concordance of the disc material used to the design specification. Disc material average hardness was 26 HRC which falls within the design limits. Fractography evaluation was carried out on the rotor disc exposed crack surface using scanning electronic microscopy (SEM) to determine the origin of the fracture.

Fig. 8 shows the crack initiation zone where intergranular crack initiation and propagation was found which is typical of a SCC failure mechanism, and Figs. 9 and 10 show the detail of intergranular crack propagation. Multiple crack branching was found along grain boundaries. Secondary crack length exceeded 1 mm. Many of the cracks were full of iron oxide. Blade fracture initiated in corrosion pits (Fig. 8). An Energy Dispersion Spectrum (EDS) of deposits found on disc fracture surfaces is shown in Fig. 11 and reveals the presence of Na, Al, S and Zn, among which Na and S are principal corrosive agents. The presence of sodium on crack surfaces indicates caustic-induced stress-corrosion cracking.

IV. Rotor Disc Failure Analysis

After analyzing details of the features recorded in rotor disc failure mechanisms as presented above, it maybe concluded that failure origin/initiation and propagation can be attributed to stress corrosion cracking (SCC). Metallurgical investigation results revealed that fracture initiation points were localized in corrosion pits that raise local stresses compared to the original unaltered surface. Corrosion products (deposits) were also found in the same zone. The presence of sodium on crack surfaces is indicative of caustic-induced stress-corrosion cracking. Also, intergranular crack initiation and propagation was found which is typical of the SCC failure mechanism.

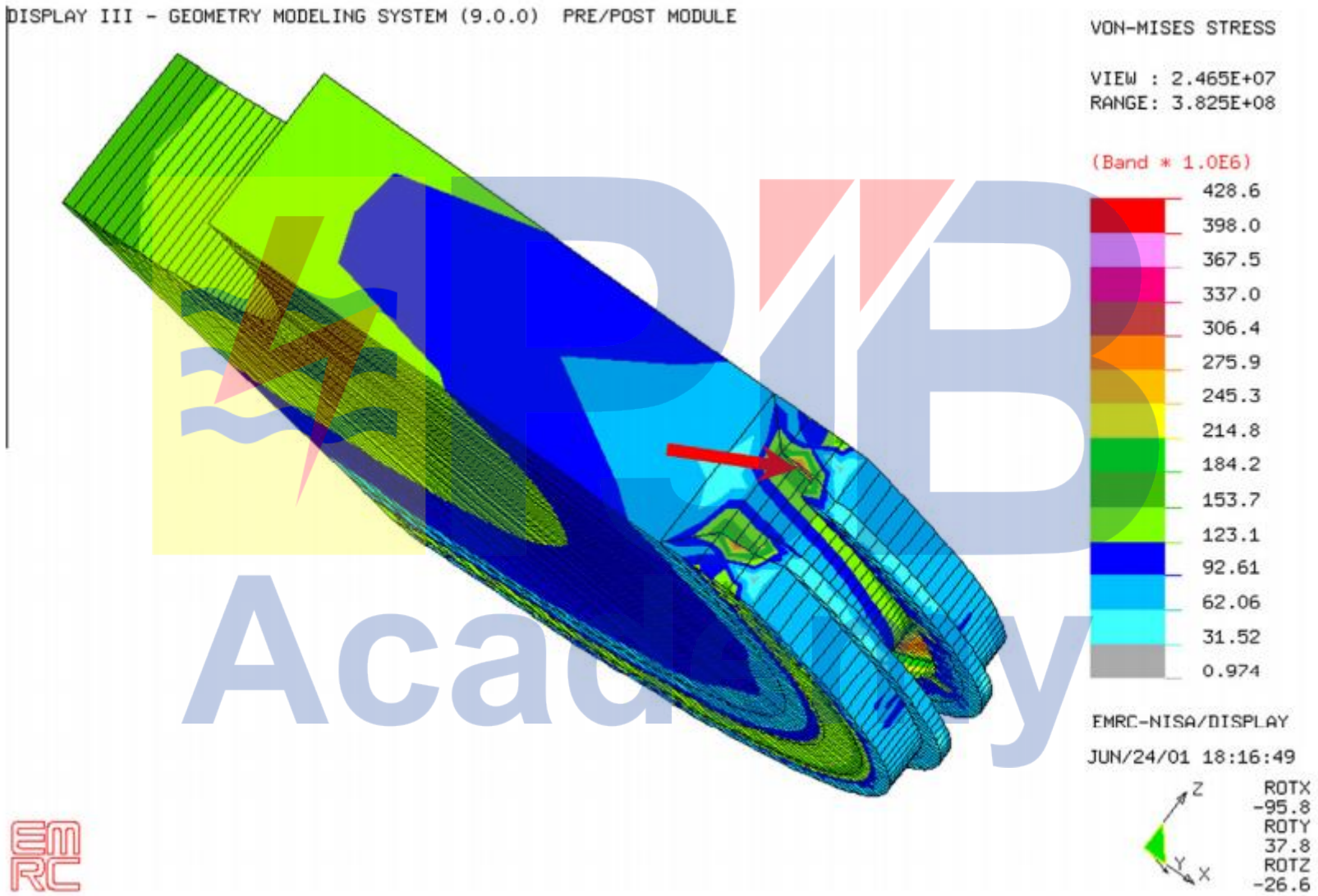

Fig. 5. Centrifugal stress distribution on the disc stage L-4. The maximum stress is R_a = 367 MPa.

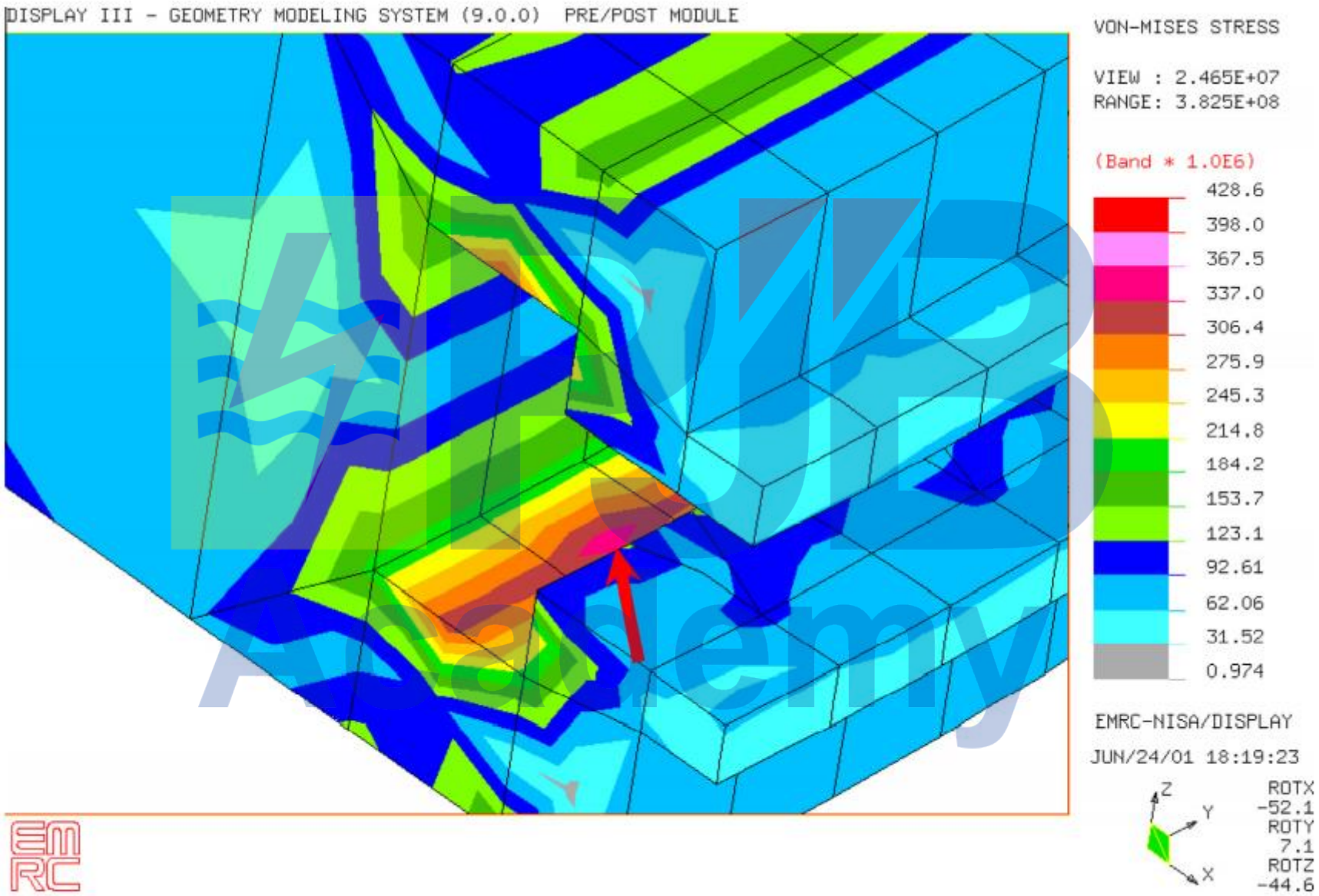

Fig. 6. Detail of maximum stress in the disc stage L-4.

Fig. 7. Rotor disc fracture surface.

In general the conditions necessary for SCC initiation are the following:

- A susceptible material.
- Presence of tensile stresses.
- Aggressive environment.

Additionally the main SCC parameters identified by David et al. [9] and Rosario et al. [10] are:

- Water composition.
- Material yield strength.
- Applied stress levels.

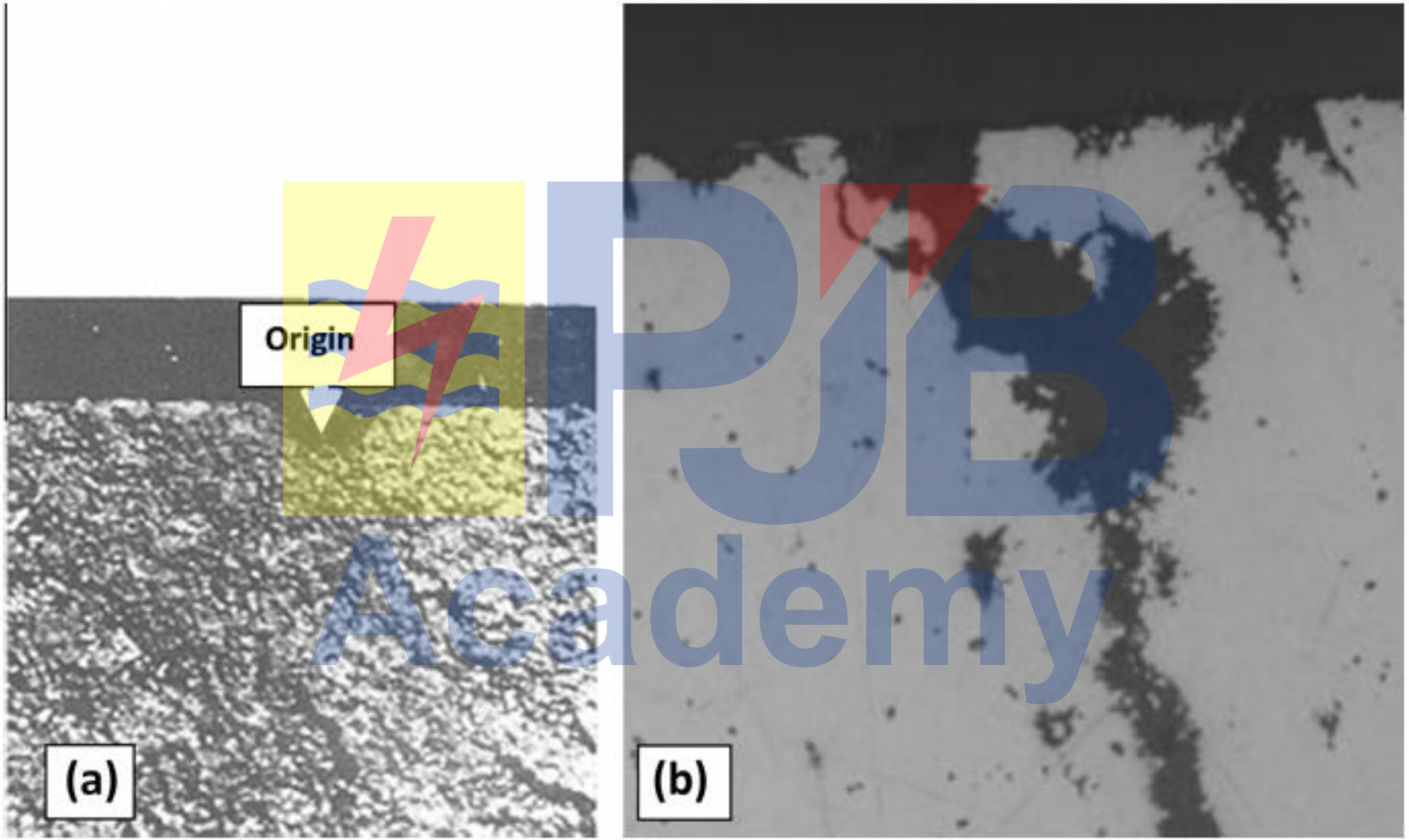

Fig. 8. Fracture origin. (a) General view, and (b) detail of fracture origin.

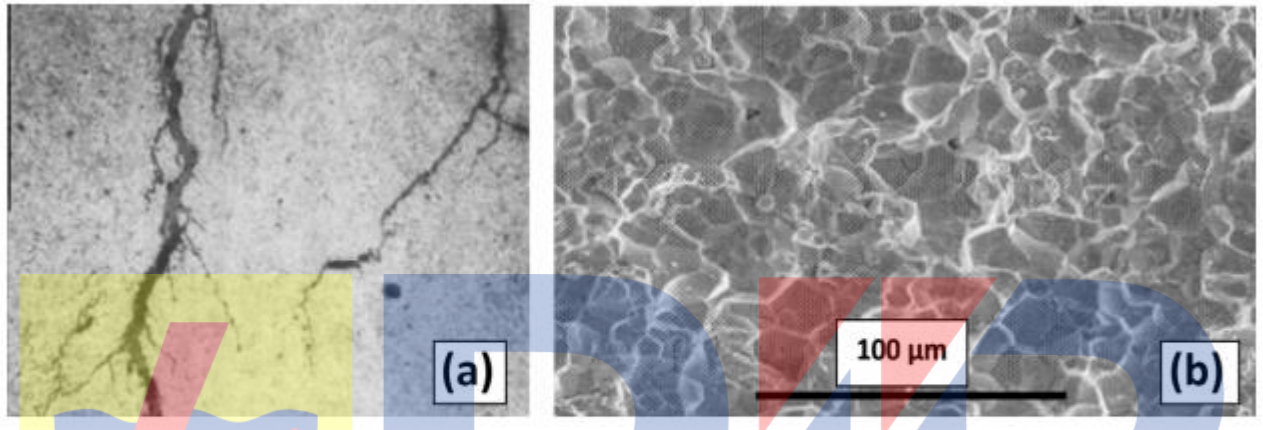

Fig. 9. Intergranular crack propagation. (a) Multiple crack branching, and (b) crack propagation.

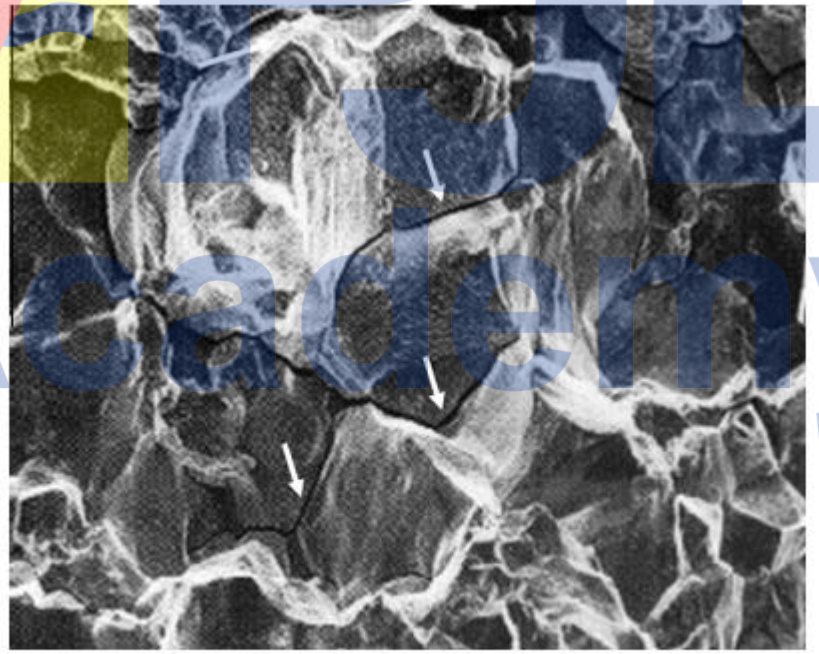

Fig. 10. Intergranular cracking (SEM).

In general low alloyed steels as in the case of these analyzed rotor discs do not have sufficient corrosion resistance when operated in humid environments.

The calculated results presented previously in Section 3, rotor actual maximum tensile stress Ra (Ra = 367 MPa) is lower than the rotor material yield strength R0.2Y.S. (R0.2Y.S. = 689 MPa). The ratio/relation between both is denominated RSCCI (stress corrosion crack initiation factor) [9] and, in this case, RSCCI = Ra/R0.2Y.S. = 0.53. According to [9] if RSCCI is within the range 0.5 < RSCCI < 0.9 and severe corrosion conditions are present, stress corrosion cracking may initiate.

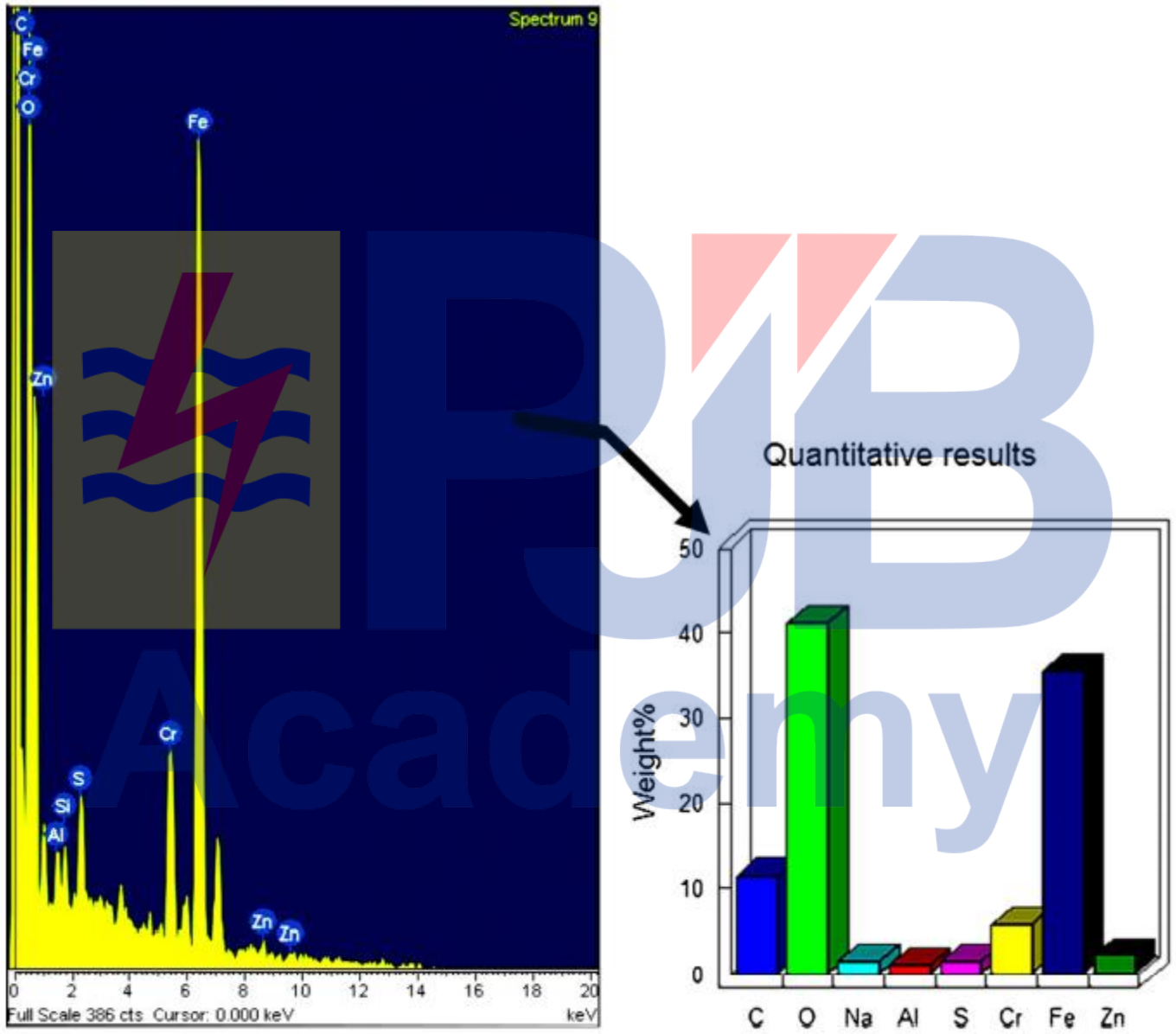

Fig. 11. An Energy Dispersion Spectrum of deposits found on disc fracture surfaces. (a) Energy Dispersion Spectrum, and (b) chemical composition.

Consider that this turbine rotor had accumulated 332,000 operation hours (40 years) until rotor disc circumferential cracks extended up to 350 mm approximately. This may be attributed to the relatively low stress corrosion crack initiation factor (RSCCI = 0.53) and not too aggressive rotor operation, as commonly steam turbine low pressure rotors operate in condensing steam (Wilson line) which cause moderate rotor corrosion.

The ultimate objective of the analysis of the failed component is to be certain that the repair to the component is optimized to prevent reoccurrence of the failure. In many cases, the repair alone cannot eliminate the failure cause. For example, a weld repair shop has little control over the steam quality at the rotor´s home power plant. However, there are incremental improvements to reliability that can be engineered into the repair. Some of these improvements can be in the mechanical design and some could be in the machining. Properties can also be optimized by choosing welding processes, filler compositions, and heat treatments that optimize the metallurgical property most affecting the prior failure mode.

In most cases a repair of a rotor is considered a ‘‘permanent’’ repair and the component is returned in ‘‘like new’’ condition to operation without restriction. However, prudent engineering practice dictates some type of post repair surveillance program of the rotor. The post repair surveillance usually consists of two separate activities: an ongoing passive vibration analysis and periodic nondestructive inspection. For rotor repair a specialized welding technique was developed based on submerged arc welding process (SA), post weld heat treatment, machining as well as a high quality non-destructive examination.

6.1. Welding process

Before the repair process, L-3 and L-4 discs were cleaned and inspected by magnetic particle methods in order to check for cracks. Other than the damaged zones, no rejectable indications were found. The discs were also inspected for oxidation and possible softening. A hardness measurement test of the discs was carried out. No unusual hardness readings were noted, nor was oxidation found. Average disc material hardness was 26 HRC. Then the damaged L-3 and L-4 discs were removed by turning to below the blade groove depth inside the disc body. The main goal of this preparation was to maintain the weld deposit heat affected zone inside the disc body. In this manner the weld-weakened zone was placed outside of the disc groove, without groove debilitation.

Build-up welding was therefore performed with an AWS A5.23-2007 EM2 filler metal, 3/3200 (2.4 mm) diameter, using a SA (Submerged Arc) welding process. The used flux was F7A8-EM2; Lincoln Electric 888.

In order to prevent carbon diffusion from the disc to the build-up material, which would result in disc softening and build-up material embrittlement, a special welding technique was used which avoids these two phenomena; Fig. 12. Welding was carried out with the rotor in a horizontal position on the facility specially adapted for SA welding. The disc was preheated by gas flame to 232-315 C in preparation for welding. The first weld beads were deposited on the base metal with low heat input-small diameter electrodes 1/1600 (1.6 mm) to "butter" the surface before any welds were made; Fig. 12. This technique reduces weld strain (distortion) and stress by preventing the formation of martensite in the base metal. 50% of bead overlap was set up. The second and following weld bead layers were deposited with adjusted weld speed to provide the correct heat input ratio for the two layers. Welding heat input and overlapping during deposition caused tempering (refining) of the bead below it (first layer).

The fine grain temperature band of the second layer tempers a coarse grain band of the first bead. This two layer HAZ refinement technique eliminates stress relief cracking and successfully improves HAZ toughness. A numerical study of the repair process compared with experimental results is presented in previous authors' investigations [11,12]. The L-4 disc SA welding process is shown in Fig. 13. Before disc welding deposition, a simulation of the welding procedure was performed on a disc sample. Various sections of the base metal, weld metal and heat affected zone were destructively tested. The mechanical property test results shown in Table 1 fell within acceptable limits. After the welding process had been completed, the disc weld zone was then machined (see Fig. 14) in preparation for bulk weldment ultrasonic inspection and weld surface magnetic particle inspection. No significant indications were found at the fusion boundaries or within the weld metal.

6.2. Stress relieving

Disc welded zones after welding were subjected to stress relief by induction heating. The rotor was hung vertically, covered by heating segments and insulated by ceramic blankets as shown in Fig. 15. Rotor expansion and bowing was monitored by a dial indicator at the bottom part. Rotor temperature was monitored by 24 thermocouples (12 thermocouples installed at each welded disc). The rotor was heated 9 h at 620 C.

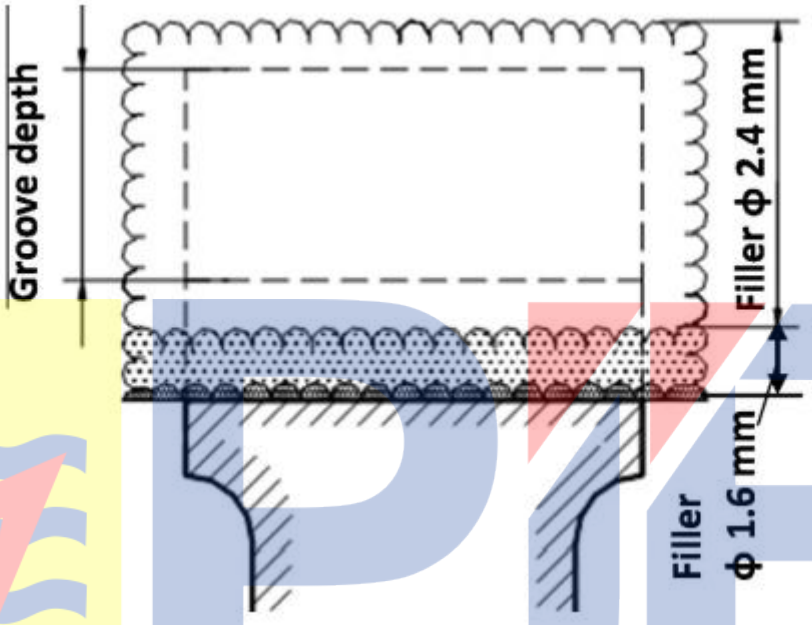

Fig. 12. Rotor disc build-up welding technique.

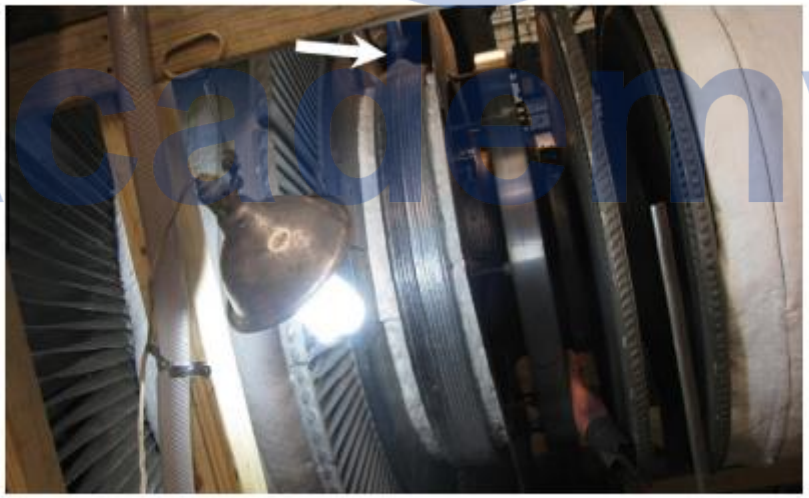

Fig. 13. The disc SA welding process.

Table 1
Mechanical properties of welding tests.

	Specificación ASTM A471-3	Base metal	HAZ	Weld
Tensile strength (MPa)	690–825	814	–	760
Yield point 0.2% (MPa)	760	703	–	690
Elongation (%)	18	21	–	24
Hardness (HB)	–	258	302	250
Impact Charpy (J)	61	85	100	120

Fig. 14. L-3 and L-4 discs rough machined after welding had been completed.

Fig. 15. Welded discs stress relieving.

After welded disc stress relief, the weldment bulk was non-destructively tested employing magnetic particle and ultrasonic techniques. This examination did not reveal the presence of any significant defects. To verify that repair welding and heat treatment had produced the desired microstructure within the weldment, an in-situ examination was undertaken following complete repair. This examination comprised metallography and hardness testing. Metallographic examination at the welded disc surface proved that the weld metal had a bainitic microstructure similar to that of the rotor disc forgings comprised of fine grained bainite. Hardness tests were conducted on the disc surface at various weldment regions using a portable dynamic instrument. The results were consistent with those on the disc forgings (base metal).

6.3. Disc Machining

Finally, the rotor was placed on the lathe and blade grooves machined in discs L-4 and L-3 to recover their original geometry. After new blade installation, rotor balancing and a run-out check, the rotor was returned to service.

VII. Rotor Disc Failure Analysis

This paper describes a case history of the failure evaluation and weld build-up repair process of 84 MW steam turbine rotor L-3 and L-4 discs that had been damaged by stress corrosion. Analyzing details of the features recorded in the rotor disc failure mechanism presented above, it may be concluded that failure origin/initiation and propagation can be attributed to stress corrosion cracking (SCC). Metallurgical investigation results revealed that fracture initiation points were localized in corrosion pits that raise local stresses compared to the original unaltered surface. Corrosion products (deposits) were also found in the same zone. The presence of sodium on crack surfaces is indicative of caustic-induced stress-corrosion cracking. Also, intergranular crack initiation and propagation was found that is typical of a SCC failure mechanism.

The stress corrosion crack initiation factor calculated value RSCCI = 0.53 and the humid ambient steam turbine rotor operation support the conclusion that stress corrosion cracking could be initiated. The weld repair of 84 MW steam turbine rotor discs has been successfully undertaken. Rotor operation success relied heavily on the specialized welding technique that was developed, as well as a high quality non-destructive examination. Weld process qualification before rotor repair should include a mock-up weld repair, metallographic examination and mechanical properties tests.

References

[1] Cottis RA. Stress corrosion cracking, guides to good practice in corrosion control. UK: National Physical Laboratory; 2000.

[2] Matocha K, Cizek P, Kauder L, Pustejovsky P. Resistance of 10GN2MFA – a low alloy steel to stress corrosion cracking in high temperature water. Nucl

Power-Control, Reliab Human Factors 2011 [ISBN: 978-953-307-599-0, InTech].

[3] Fraser FW, Metzbower EA. Fractographic and microstructural analyses of stress corrosion cracking in HY-130 weldments. In: 62nd AWS annual

meeting. Ohio: Cleveland; 1981.

[4] Kramer E, Huber H, Scarlin B. ABB Rev 1996;5.

[5] Reid SR, Golden G. SCC of low pressure rotor blade attachments. Energy Technol 2013.

[6] Wasuthalainan K, Nangkala K. Stress corrosion cracking on steam turbine rotor grooves: experiences and countermeasures from EGAT powerplants. Bangkok Thailand: Power-Gen Asia; 2009.

This repair procedure can also be applied to to the rotor disc failure which occurs in Indonesia as presented previously.

[7] NISA module, Engineering Mechanics Research Corporation; 2000.

[8] Results of the material testing: rotor for 84,000 kW turbine, Nagasaki Steel Works; 1970.

[9] David W, Rottger G, Schleithoff K, Hamel H, Termuehlen H. Disk-type LP turbine rotor experience, in pressurised water reactors. The steam turbine

generator today: materials, flow path design, repair, and refurbishment, vol. 21. ASME; 1993. p. 83–92.

[10] Rosario D, Viswanathan R, Wells C, Licina G. Stress corrosion cracking of steam turbine rotors. Corrosion 1998;54(7):531–45.

[11] Mazur Z, Salazar O, González G, Urquiza G. Numerical prediction of heat affected zone (HAZ) grain refinement for multiples weld-beads deposits

during SMAW welding process of Cr–Mo–V steel. Revista de Metalurgia 2001;37:563–72.

[12] Mazur Z, Gonzalez G, Urquiza G, Salazar O, Mariño C, Hernández A. Numerical prediction of the microstructure of weld heat affected zone (HAZ) in

SMAW weld deposits on Cr–Mo–V steel. Revista de Metalurgia 2002;38:14–22.